Proceedings of the 8th U.S. National Conference on Earthquake Engineering
April 18-22, 2006, San Francisco, California, USA
Paper No. 239

PROOF-OF-CONCEPT TESTING AND FINITE ELEMENT MODELLING OF SELF-STABILIZING HYBRID RECTANGULAR LINKS FOR ECCENTRICALLY BRACED FRAMES

J. W. Berman[1] and M. Bruneau[2]

ABSTRACT

This paper describes the design, testing, and finite element modeling, of a proof-of-concept eccentrically braced frame specimen utilizing a hybrid rectangular shear link. The link is self-stabilizing and does not require lateral bracing, making it suitable for use in steel bridge piers where lateral bracing can be difficult to provide (building applications are possible as well). Equations used for design are given and references for their derivations are provided. The quasi-static cyclic testing is described, and results are reported and compared with a finite element model to be used as the basis for a future parametric study. Stable and full hysteretic loops were obtained and no signs of flange, web, or lateral torsional buckling were observed. The link was subjected to 0.15 radians of rotation in the final cycle, which is almost twice the maximum rotation allowed in building codes for links with I-shaped cross-sections. Although the final failure mode was fracture of the bottom link flange, the large rotations achieved were well above what would be required in a seismic event, indicating that hybrid rectangular links without lateral bracing of the link can indeed be a viable alternative for applications in steel bridge piers in seismic regions.

Introduction

Eccentrically braced frames (EBFs) have been shown to exhibit excellent seismic performance (Roeder and Popov (1977), Hjelmstad and Popov (1983), Kasai and Popov (1986), Engelhardt and Popov (1989), among others). However, they have had limited use in steel bridge piers in part because of the difficulty in providing the lateral bracing required to prevent lateral torsional buckling of the link. Therefore, the development of an EBF system where lateral bracing of the link is not necessary would be desirable in the context of seismic design and retrofit of bridges.

[1] Ph.D. Candidate, Department of Civil, Structural, and Environmental Engineering, 130 Ketter Hall, University at Buffalo, Buffalo, NY 14260; email: jwberman@eng.buffalo.edu
[2] Director, Multidisciplinary Center for Earthquake Engineering Research and Professor, Department of Civil, Structural, and Environmental Engineering, 130 Ketter Hall, University at Buffalo, Buffalo, NY 14260; email: bruneau@mceermail.buffalo.edu

From this motivation, the concept of an EBF utilizing a rectangular hybrid cross-section for the link is explored (hybrid in this case meaning the yield stresses of the webs and flanges may be different), as rectangular cross-sections inherently have more torsional stability than I-shaped cross-sections and may not require lateral bracing. First, link design is discussed in terms of plastic shear force and moment, normalized link length, and compactness and stiffener requirements, and references are provided. Then, the specimen and test setup are described. Experimental results are discussed and compared with the results of finite element modeling of the link.

Design of Hybrid Rectangular Links

A link with a hybrid rectangular cross-section is shown in Fig. 1. Assuming the moment on the section is less than the reduced plastic moment (described below), the plastic shear force, V_p, for the cross-section is (Berman and Bruneau, 2005):

$$V_p = \frac{2}{\sqrt{3}} F_{yw} t_w \left(d - 2t_f\right) \tag{1}$$

where F_{yw} is the yield stress of the webs, t_w is the web thickness, d is the depth of the section, and t_f is the flange thickness. The plastic moment, M_p, for the cross-section shown in figure is:

$$M_p = F_{yf} t_f \left(b - 2t_w\right)\left(d - t_f\right) + F_{yw} \frac{t_w d^2}{2} \tag{2}$$

where F_{yf} is the yield stress of the flanges, b is the section width, and other terms are as previously defined. This plastic moment may also be reduced for the presence of the plastic shear force, as a simple way of accounting for shear-moment interaction in the presence of the full plastic shear. The reduced plastic moment, M_{pr}, can be written as:

$$M_{pr} = F_{yf} t_f \left(b - 2t_w\right)\left(d - t_f\right) + 2F_{yw} t_f t_w \left(d - t_f\right) \tag{3}$$

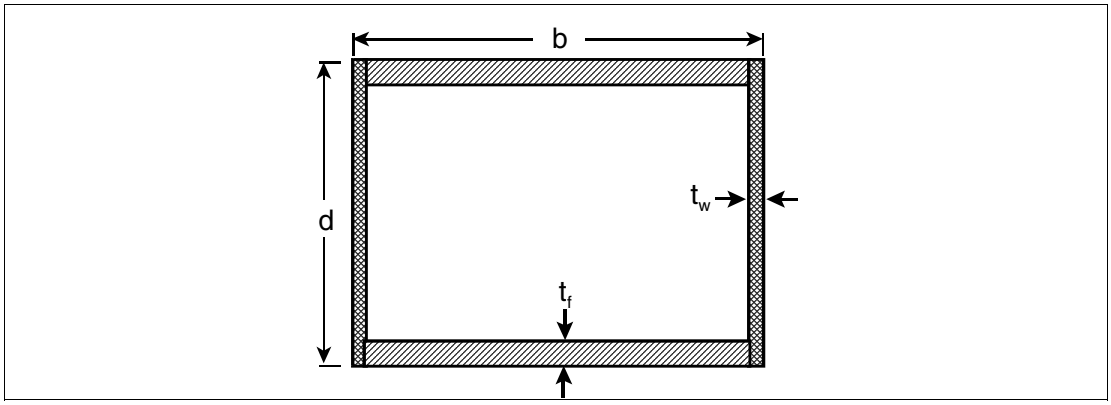

Figure 1. General hybrid rectangular link cross-section.

As with links having I-shaped cross-sections, hybrid links with rectangular cross-sections fall into one of three categories, shear links, intermediate links, and flexural links. Classification of links can be done using the normalized link length, ρ, defined as $e/(M_p/V_p)$, where e is the link length. Links having $\rho \leq 1.6$ are shear links and the inelastic behavior is dominated by shear yielding of the webs. Links having $1.6 < \rho \leq 2.6$ are intermediate links, for which inelastic

behavior is a mix of shear and flexural behavior, and links having $\rho > 2.6$ are flexural links where inelastic behavior is dominated by flexural yielding. These ranges are the same as those for I-shaped links, since there is no expected difference in the factors used to determine them, namely, overstrength and strain hardening (Berman and Bruneau, 2005). For I-shaped links, the AISC Seismic Provisions (AISC, 2002) limit the inelastic link rotation for shear links and flexural links to 0.08 rads and 0.02 rads, respectively, with linear interpolation based on normalized link length to be used for intermediate links. At this point there is no data indicating these limits should be different for hybrid rectangular links.

The necessity for using hybrid rectangular cross-sections arises from the short link lengths, and therefore high stiffness, required for HSS shapes that are listed in the AISC LRFD Manual of Steel Construction to be shear links (i.e. have $\rho \leq 1.6$). For example, the maximum length for a shear link, that also meets the compactness limits, would be 460 mm and would be obtained with a HSS 250x250x16. Considering a 7.3 m wide by 3.7 m tall frame, the drift at a plastic rotation of 0.08 rads is only 0.5% from (Bruneau et al., 1998):

$$\theta = \gamma \frac{e}{L} \tag{4}$$

Compactness limits for webs and flanges of hybrid rectangular links, as well as stiffener spacing requirements, are derived in Berman and Bruneau (2005) and are summarized here as follows:

- Flanges should have $b'/t_f \leq 0.64\sqrt{E_s/F_{yf}}$, where $b' = b\text{-}2t_w$.
- For shear links webs should have $d'/t_w \leq 1.67\sqrt{E_s/F_{yw}}$ and webs with $d'/t_w \leq 0.64\sqrt{E_s/F_{yw}}$ may be used without stiffeners, where $d' = d\text{-}2t_f$.
- Stiffeners for shear links should have a spacing, a, satisfying:
  $$\frac{a}{t_w} + \frac{1}{8}\frac{d}{t_w} = C_B \tag{5}$$
  where C_B is 20 and 37 for anticipated maximum link rotations of 0.08 rads and 0.02 rads respectively.
- For intermediate and flexural links webs should have $d'/t_w \leq 0.64\sqrt{E_s/F_{yw}}$.

For stiffener strength and size requirements the reader is referred to Berman and Bruneau (2005).

Proof-of-Concept Test Setup

The proof-of-concept EBF with a hybrid rectangular shear link was designed to be as large as possible considering the constraints of the available equipment in the Structural Engineering and Earthquake Simulation Laboratory (SEESL) at the University at Buffalo (UB). Quasi-static cyclic loading per ATC-24 (ATC, 1992) was chosen and the maximum force output of the actuator available (1115 kN) was divided by 2.5 to account for the possibility of obtaining material with a higher than specified yield stress as well as strain hardening, making the design base shear 445 kN. The general test setup is shown in Fig. 2. Assuming the moments at the middle of the link and clevises are zero, the design link shear can be found to be 327 kN for the

dimensions shown. To design the link, the equations described above were used in conjunction with enforcing a minimum link length such that a drift of at least 1% corresponds to a maximum link rotation of 0.08 rads and assuring $\rho < 1.6$ (i.e., maintaining a shear link). The selected link dimensions were: $d = b = 150$ mm, $t_f = 16$ mm, $t_w = 8$ mm, and $e = 460$ mm. Link stiffeners were placed at a spacing of 152 mm and were 13 mm thick and attached with fillet welds. A steel yield stress of 345 MPa was assumed during the design process and ASTM A572 Gr. 50 steel was specified for fabrication of the link beam which gave an anticipated link shear of 381 kN.

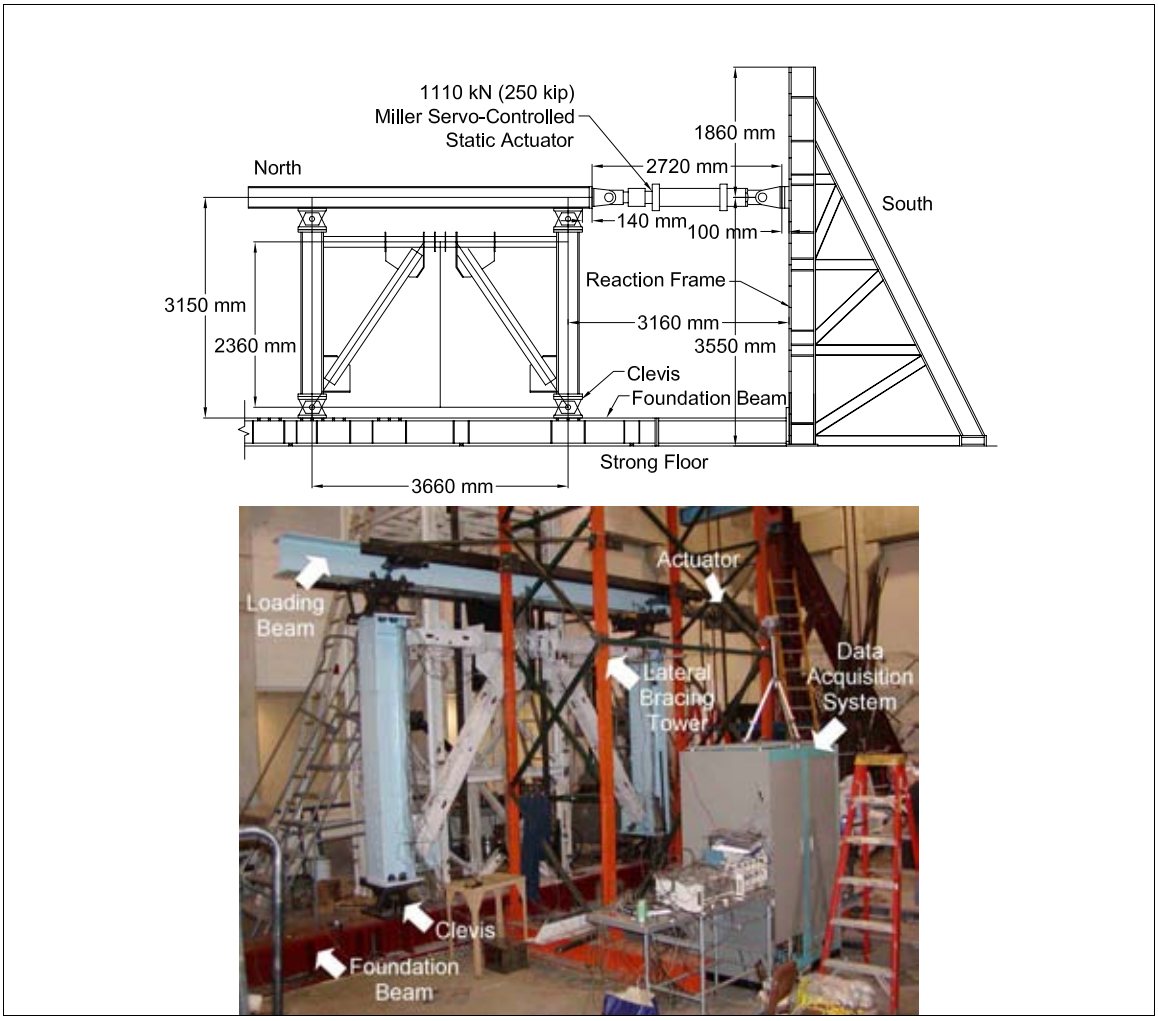

Figure 2. Proof-of-concept test setup.

The framing outside the link was designed using capacity principles. Factors to account for the difference between specified and expected (i.e., mean) yield stress of the link material as well as strain hardening were incorporated, resulting in the member sizes shown in Fig. 3.

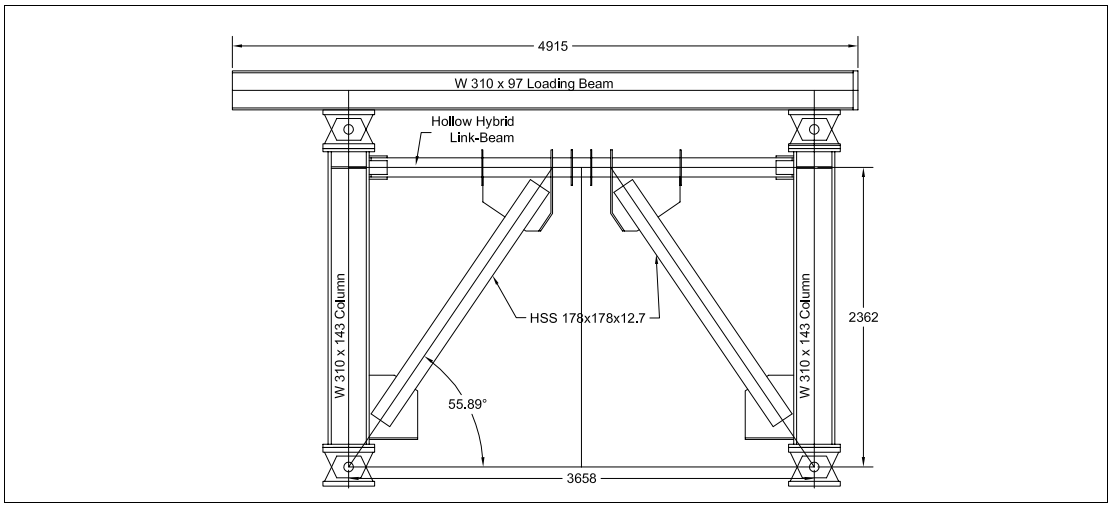

Figure 3. Test specimen with dimensions.

Experimental Results

The experimentally obtained base shear versus frame drift hysteresis is shown in Figure 4a and the link shear force versus link rotation hysteresis is shown in Figure 4b. From the elastic cycles of Figure 4a, the initial stiffness of the specimen was found to be 80 kN/mm. The yield base shear and frame drift were 668 kN and 0.37% while the maximum base shear and drift were 1009 kN and 2.3%, respectively. Link shear force and rotation at yield were 490 kN and 0.014, while the maximum link shear and rotation achieved were 742 kN and 0.151 rads, respectively. Projecting the elastic and inelastic slopes of Figure 4b leads to an approximation of the plastic link shear force of 520 kN. The link shear force at 0.08 rads of rotation (the current limit for shear links) was 689 kN. Assuming equal link end moments, the end moments at specimen yield, development of Vp, and 0.08 rads of rotation were 112 kN-m, 119 kN-m, and 158 kN-m, respectively, and the maximum link end moment was 170 kN-m.

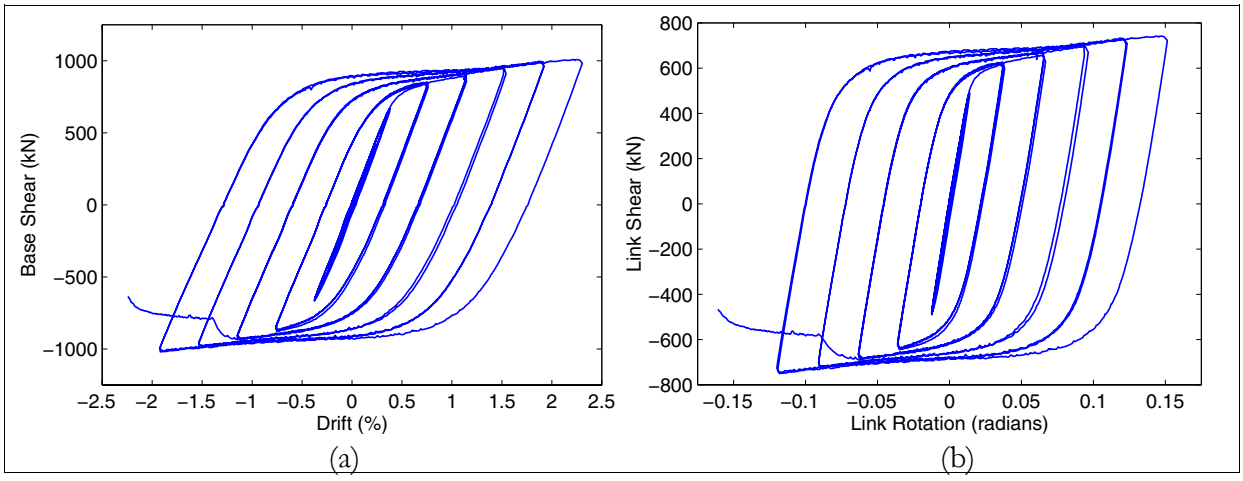

Figure 4. (a) Base shear versus frame drift (b) Link shear versus link rotation.

The link achieved a rotation level 0.151 rads, which is almost twice the current limit for shear links in EBF for buildings (0.08 rads) and the target rotation for the specimen. Furthermore, the EBF reached a frame displacement ductility 6.0 and link rotation ductility of over 10 (the difference in these is due to the flexibility of the surrounding framing). Figure 5a shows the deformed link at 0.123 rads (1.92% drift) during Cycle 19.

Link failure occurred when the bottom flange at the north end of the link fractured as shown in Figure 5b. The fracture occurred in the heat affected zone (HAZ) of the flange adjacent to the fillet weld connecting the gusset stiffener of the brace-to-link connection to the link. Inspection of the failure surface was performed using a magnifying glass and light-microscope with 30x magnification (personal communication, Mark Lukowski, metallurgist, and Dr. Robert C. Wetherhold, mechanical engineer, Department of Mechanical and Aerospace Engineering, University at Buffalo, September 2003). The fracture was assessed as having initiated by cracking in the previously described HAZ and the propagation of those cracks under load reversals. There was no evidence of crack initiation in the full penetration groove weld used to assemble the webs and flanges of the link.

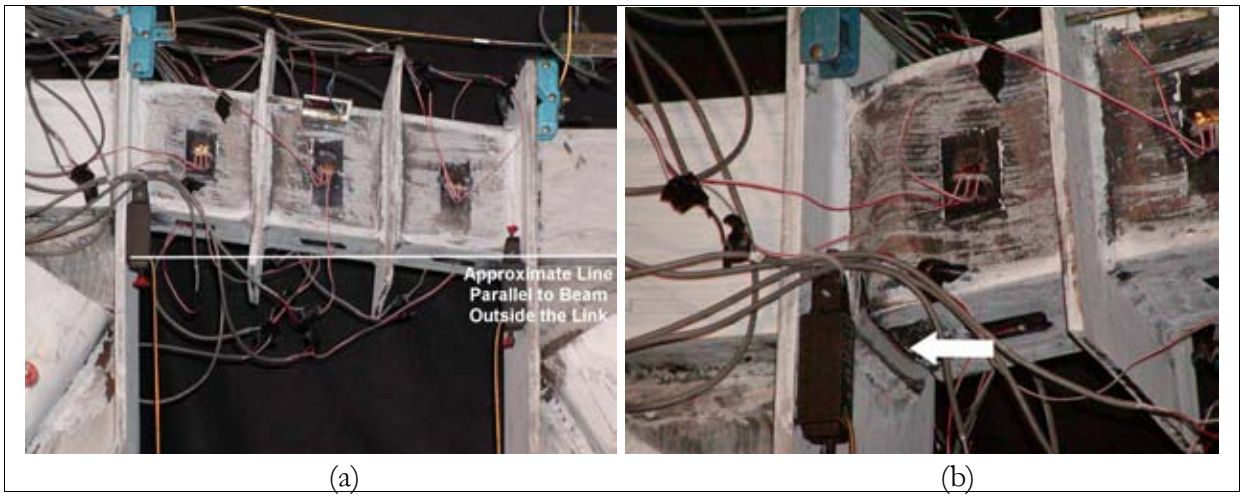

Figure 5. (a) Link deformed at 0.123 rads of rotation during cycle 19 (b) Fractured bottom flange at north end of link.

Finite Element Modeling of Proof-of-Concept Link

A finite element model of the link from the proof-of-concept test was developed in ABAQUS (HKS, 2001). Some preliminary analyses were conducted to study the effect of mesh refinement and to determine whether reduced integration elements could be used to improve computational time without loss of significant accuracy.

The finite element model used shell elements to represent the webs, flanges, and stiffeners of the proof-of-concept link. An element edge length of approximately 25 mm was found to adequately represent the behavior of the link through a mesh refinement study. The resulting element edge to thickness ratios varied from 1.6 to 3.0. Reduced integration shell elements denoted S4R in ABAQUS were selected to improve computation time and were found

to have no noticeable impact on the results. Computation time is important because this model will serve as the basis for a finite element parametric study of different link geometries in future work. The resulting model is shown in Fig. 6.

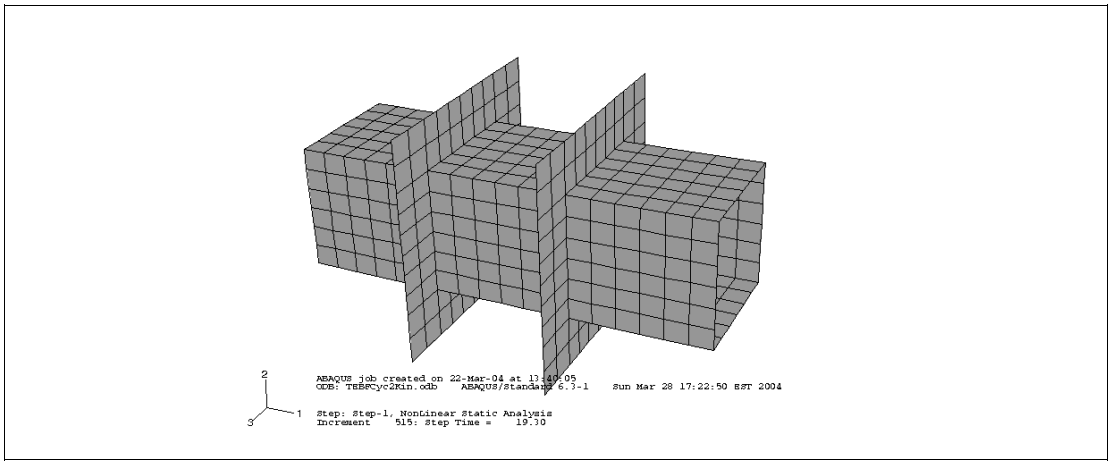

Figure 6. Final mesh for finite element model of proof-of-concept link.

Boundary conditions similar to those employed by Richard and Uang in their study of wide-flange links were used here and are shown schematically in Fig. 7. These boundary conditions allow axial deformation of the link while preventing rotation at both ends, similar to the boundary conditions for the proof-of-concept link specimen.

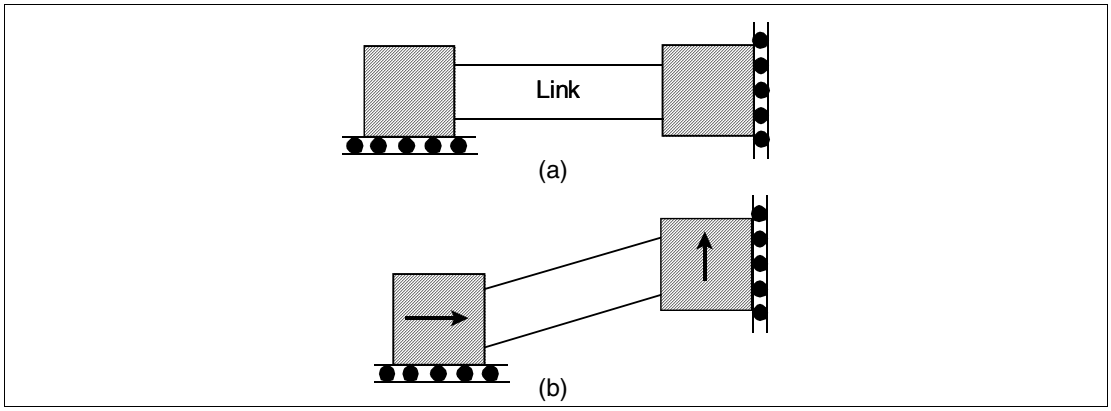

Figure 7. Link boundary conditions for: (a) the undeformed configuration and (b) the deformed configuration (adapted from Richards and Uang, 2002).

The nonlinear kinematic hardening plasticity material model available in ABAQUS was used in the finite element model of the proof-of-concept link. Only monotonic coupon test data was available for the materials used to fabricate the link, therefore these were input as half cycle data for the material model. The experimental stress-strain curve and ABAQUS stress strain curves are shown in Figs. 8 and 8b for the web and flange material respectively. The flange material definition was also used for the stiffeners.

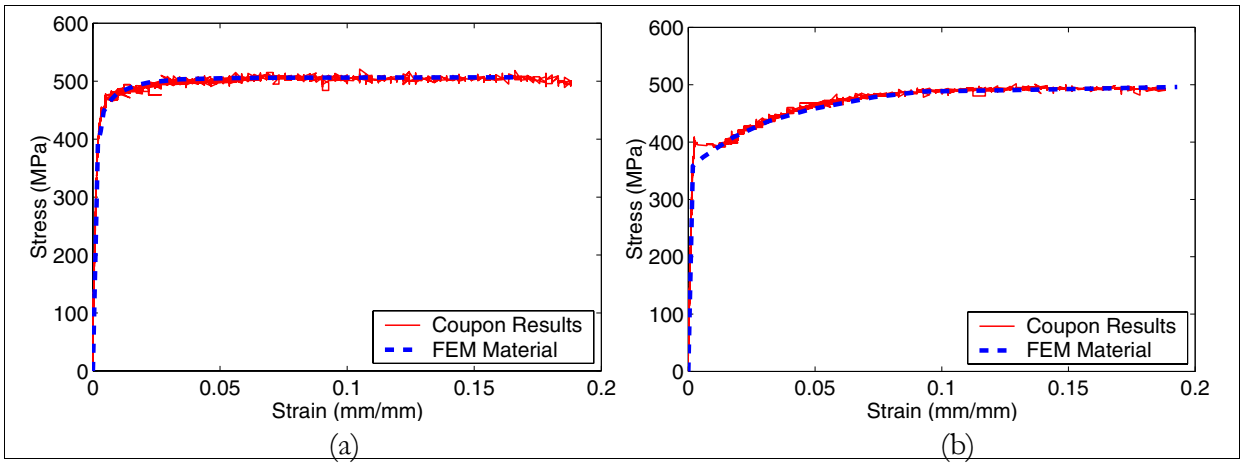

Figure 8. Stress strain curves from experimental results and for for ABAQUS material definitions for: (a) the link web and (b) the link flange.

As shown in Figs. 9 and 10, good agreement was obtained between the analytical and experimental results in terms of both hysteretic behavior and overall deformation pattern. Stresses and strains at key locations in the finite element model were also near expected values. Given these results, this model will serve as the basis for a finite element parametric study that will investigate limiting compactness ratios, stiffener requirements, effect of link length, energy dissipation, and overstrength of hybrid rectangular links for eccentrically braced frames.

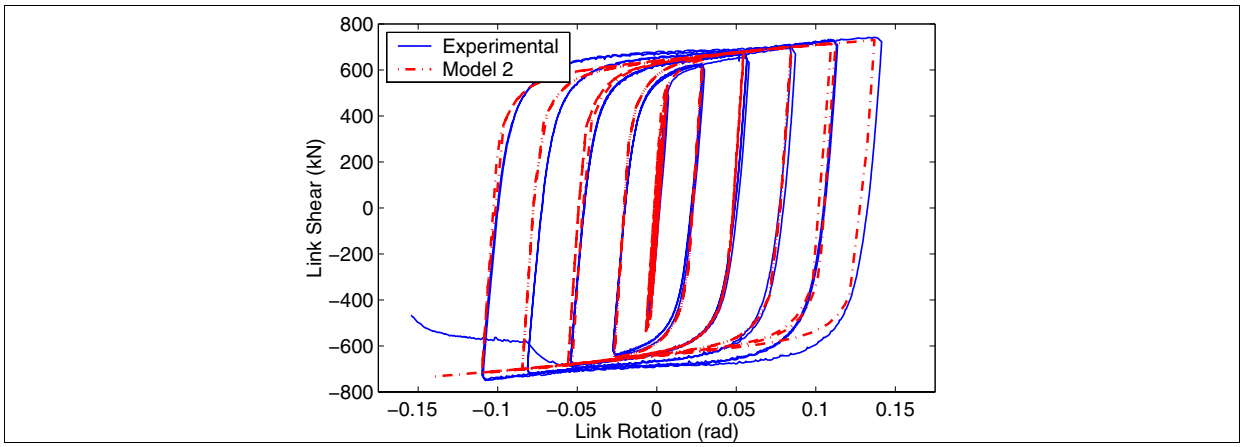

Figure 9. Comparison of experimental and analytical hystereses (model 2 indicates the second mesh refinement.

Conclusions

A new link for eccentrically braced frames that is self-stabilizing and does not require lateral bracing has been developed, tested, and modeled analytically. The results indicate that hybrid rectangular shear links can achieve ductility levels similar or larger than those reached in testing of wide-flange links. Design equations and requirements have been proposed and, in a preliminary sense, verified by the successful testing of the proof-of-concept specimen.

Comparison with a finite element model showed reasonable agreement in terms of deformations and hysteretic behavior. This model will be used in a future parametric study to further investigate the adequacy of the proposed design requirements.

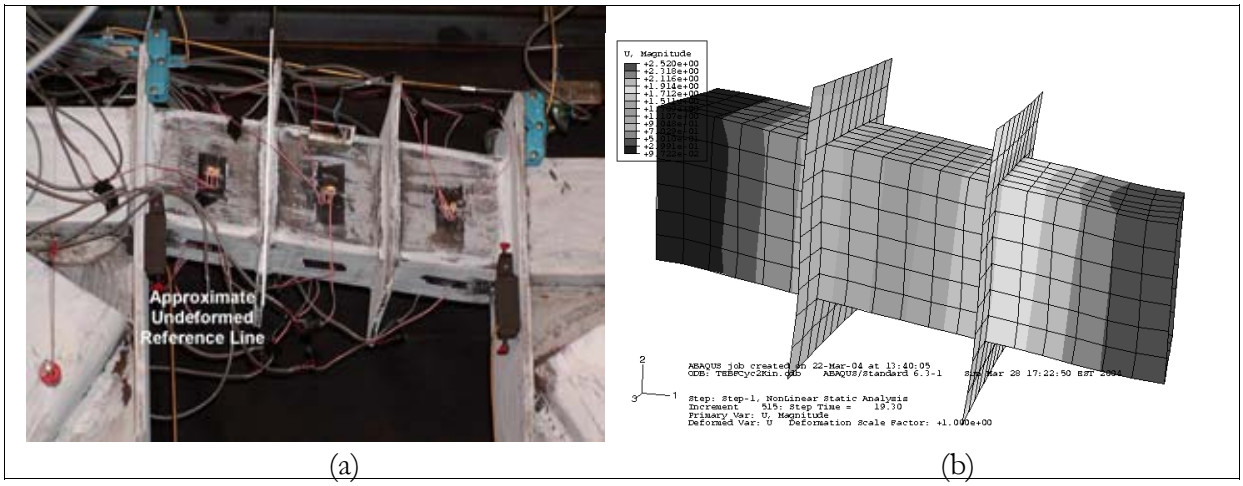

Figure 10. Comparison of experimental and analytical link deformations at similar rotation levels.

Acknowledgments

This research was conducted by the State University of New York at Buffalo and was supported by the Federal Highway Administration under contract number DTFH61-98-C-00094 to the Multidisciplinary Center for Earthquake Engineering Research. However, any opinions, findings, conclusions, and recommendations presented in this paper are those of the authors and do not necessarily reflect the views of the sponsors.

References

AISC, 1998. *Manual of Steel Construction: Load and Resistance Factor Design.* 3rd Ed. American Institute of Steel Construction, Chicago, IL.

AISC, 2002. *Seismic Provisions for Structural Steel Buildings.* American Institute of Steel Construction, Chicago, IL.

ATC (1992). *Guidelines for Seismic Testing of Components of Steel Structures Report-24*, Applied Technology Council, Redwood City, CA.

Berman, J. W., and Bruneau, M., 2005. "Approaches for the Seismic Retrofit of Braced Steel Bridge Piers and Proof-of-Concept Testing of a Laterally Stable Eccentrically Braced Frame" *Technical Report MCEER-05-0004*, Multidisciplinary Center for Earthquake Engineering Research.

Bruneau, M., Uang, C.M., and Whittaker, A., 1998. *Ductile Design of Steel Structures*. McGraw-Hill, New York, NY.

Engelhardt, M.D., and Popov, E.P., 1989. "Behavior of Long Links in Eccentrically Braced Frames". *Report No. UCB/EERC-89-01*, Earthquake Engineering Research Center, College of Engineering, University of California Berkeley, Berkeley, CA.

Hjelmstad, K.D., and Popov, E.P., 1983. "Cyclic Behavior and Design of Link Beams". *Journal of Structural Engingeering*, ASCE, 109(10), 2387-2403.

HKS (2001), "ABAQUS Standard User's Manual," Hibbitt, Karlsson, and Sorensen, Inc., Pawtucket, RI.

Kasai, K., and Popov, E.P., 1986. "General Behavior of WF Steel Shear Link Beams". *Journal of Structural Engineering*, ASCE, 112(2), 362-382.

Richards, P., and Uang, C.M. (2002) "Evaluation of Rotation Capacity and Overstrength of Links in Eccentrically Braced Frames." *Report No. SSRP-2002/18*, Structural Systems Research Project, Department of Structural Engineering, University of California San Diego, La Jolla, CA.

Roeder, C.W., and Popov, E.P., 1977. "Inelastic Behavior of Eccentrically Braced Steel Frames Under Cyclic Loadings". *Report No. UCB/EERC-77/18*, Earthquake Engineering Research Center, College of Engineering, University of California Berkeley, Berkeley, CA.